

Performance profile of Cold Storage Using R32 as Refrigerant for Traditional Fishing Boat with Photovoltaic as Energi Source

Suhengki¹, Henry Munandar Manik¹, Muhamad Yulianto^{2*}, Edy Hartulistiyoso², Willi Sumatri², Hamidah³, Totok Hestirianoto¹, Susilohadi⁴

¹Department Department of Marine Science and Technology, Faculty of Marine Science and Technology, IPB University, Jalan Lingkar Akademik, Kampus IPB Dramaga, Babakan, Dramaga, Babakan, Kec. Dramaga, Kabupaten Bogor, Jawa Barat 16002, Indonesia.

²Department of Mechanical and Biosystem Engineering, Faculty of Agricultural Engineering and Technology, IPB University, Jalan Lingkar Akademik, Kampus IPB Dramaga, Babakan, Dramaga, Babakan, Kec. Dramaga, Kabupaten Bogor, Jawa Barat 16002, Indonesia

³Commissioner of PT. Samudra Sinar Abadi Shipyard. Warehousing Margomulyo Permai Blok, F No. 19 Margomulyo, Surabaya

⁴Research Center For Geological Resources-BRIN, Jalan Dr Djunjunan No 236, Husen Sastra Negara, Kec Cicendo, Kota Bandung Jawa barat Indonesia. Email : susi0@brin.go.id

*Corresponding author, email: muhamad_yulianto@apps.ipb.ac.id

Article Info

Submitted: 1th, June 2024
Revised: 15th, July 2024
Accepted: 22th, July 2024
Available online: 31, July 2024
Published: August 2024

Keywords:

Performance, Cold Storage, R32,
Photovoltaic, Fishing Vessel

How to cite

Suhengki, Manik, H. M., Yulianto, M.,
Haryulistiyoso, E., Sumantri, W., Hamidah,
Hestirianoto, T., Susilohadi. 2024.
Performance profile of Cold Storage Using
R32 as Refrigerant for Traditional Fishing
Boat with Photovoltaic as Energi Source.
Jurnal Keteknikan Pertanian, 12(2): 184-203.
<https://doi.org/10.19028/jtep.012.2.184-203>

Abstract

This paper discusses the performance of cold storage using R32 refrigerant. R32 is one of the recommended refrigerants, with the main advantages of low Global Warming Potential (ODP) and GWP (global warming potential (GWP) values of approximately 0 and 675. However, because this refrigerant is classified as a new refrigerant, its implementation is limited to air-conditioning and heat pumps. In this study, R32 was tested for cold-storage applications. The cold storage performance was studied with respect to the achieved temperature, power consumption, cooling capacity, and Coefficient of Performance without load. The testing was carried out in two ways: cold storage testing on a laboratory scale and direct testing on a 5 GT fishing boat. The performance results show that both tests on a lab scale and tests directly on a fishing boat without a load can reach a cold storage room temperature of approximately -18°C . Meanwhile, the power consumption of the compressor supplied by photovoltaic power was 0.653-0.776 kW. The other evaluation parameters, such as the cooling capacity (Q_e), heat rejection (Q_c), and COP were shown around 4,98 kW, 5,94 kW, And 7,72 respectively. Based on the test results, R32 has the potential to be applied in cold storage.

Doi: <https://doi.org/10.19028/jtep.012.2.184-203>

1. Introduction

Indonesia has an abundant potential as a marine resource. The ocean area, which covers two-thirds of Indonesia or approximately 5.9 million km², produces a potential catch of 6.4 million tons per year, as revealed by Arianto (2020). This huge potential certainly needs to be utilized as much as possible,

considering that marine biological catches include products that are easily damaged (perishable), which is certainly a problem, especially for fishermen. One of the causes of fish products caught by fishermen quickly experiencing damage is the storage method, which uses traditional methods, namely ice cubes or ice powder (slurry), which are inserted into the box. This method of storing fish has weaknesses such as the short storage time reported by Arief et al. (2021). In addition, ice melting during storage soaks the catch, which accelerates the process of catch deterioration and potentially increases the value of catch shrinkage. This limits fishermen in terms of fishing time and ice availability for storing catches. One solution to this problem is to use cold storage with a vapor-compression refrigeration system.

According to Nurhasanah and Sudarmadi (2015) and Hu et al. (2021) Vapor compression refrigeration system is a cooling system that works by evaporating the refrigerant in the evaporator to absorb heat from the surrounding environment, compressing the vapor using a compressor to increase its pressure, flowing the high-pressure vapor to the condenser to release heat to the environment, and finally flowing the refrigerant in a low-pressure liquid form through the expansion valve to return to the evaporator and repeat the cycle continuously, resulting in an efficient cooling effect. The system consists of four main components: compressor, condenser, expansion valve, and evaporator, as shown in Figure 1.

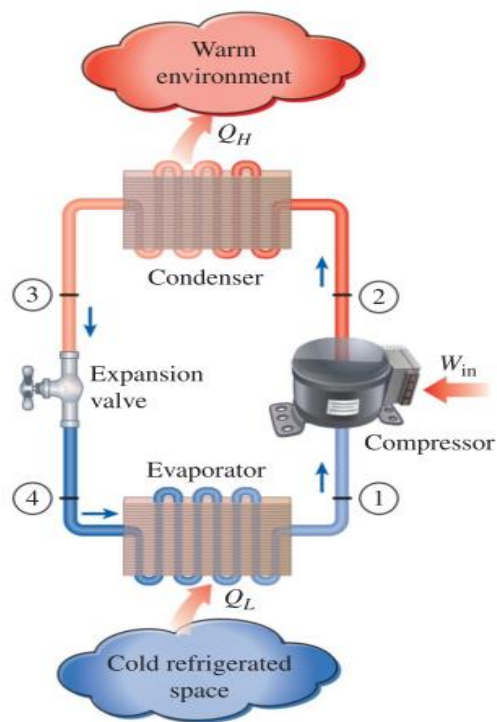


Figure 1. Components of vapor compression refrigeration system (Cengel and Boles, 2015).

Prayudi and Suhengki revealed one of the weaknesses of vapor compression refrigeration systems. (2017) and Yang et al. (2021) had high energy consumption and CO₂ contributions. Several studies related to the use of refrigerants have been conducted (Table 1). Recent research by Saito (2017) has revealed that R32 is a promising new refrigerant for heat-pump applications. Based on this, it can be seen that the use of R32 for cold storage applications has not been carried out by other researchers.

Table 1. Research related to the use of refrigerants and applications.

Reference	Refrigerant	Energy source	application	Description
Yulianto <i>et al.</i> (2024)	R32	Electric	Heat pump water heater	Mass charge have influence to the COP of heat Pump
Hadi <i>et al.</i> (2024)	R32, R134a	Electric	Heat Pump Water Heater	COP of R32 better than R134a by simulation
Yulianto <i>et al.</i> (2022)	R32	Electric	Heat Pump Water Heater	COP 5 in the tropical condition by experiment and simulation
Cabello <i>et al.</i> (2022)	R455a, R468a, R290, R1270	Electric	Refrigerator	R1270 could increasing COP 33,26% in the same condensation temperature
Zheng <i>et al.</i> (2022)	R290, R134a	Electric	Ice storage air conditioning	COP R290 almost have same value with R134 around close to 1
Fachruddin, <i>et al.</i> (2021)	R134a	Electric	cold storage	R134 have COP around 3,14 by experiment
Nengah <i>et al.</i> (2021)	R410a, R32	Electric	Air Conditioning (AC)	COP R32 is less than 4% compared to R410a, but R32 have higher cooling capacity
Giriprasath <i>et al.</i> (2021)	R32, R290	Electric	Air Conditioning (AC)	COP R32 is better than R290
Bhamidipati <i>et al.</i> (2020)	R32, R134a, R152a	Electric	Air Conditioning (AC)	R32 have the best COP around 4.13-7,12 by simulation
Pattana <i>et al.</i> (2020)	R404	Electric	Cold storage	COP around 2,29-2,47
Shi <i>et al.</i> 2019	R410a, R32	Electric	Air Conditioning (AC)	R32 have better COP using rotary compressor
Preston <i>et al.</i> (2018)	R507	Electric	Cold storage	R507 is have COP 3,43-3,76

Hidayatno et al. (2020) Indonesia had an average daily irradiation of 4.80 kWh/m² which theoretically has excellent potential as a solar energy source. A study conducted by Natarajan et al. (2023) showed that the use of photovoltaic renewable energy can reduce cold storage energy consumption by 17.9% compared to conventional cold storage.

Based on the explanation above, there is a research gap that has not been addressed by other researchers, namely, the use of R32 in cold storage equipped with an energy source from photovoltaic, which in this study will discuss its performance.

2. Materials and Methods

The refrigerant used in this study was R32. R32 is a refrigerant that has the advantage of being made from synthetic materials with low ODP and GWP values, namely, ODP = 0 and GWP = 675. The disadvantage of R32 is that it is included in the A2L category or is flammable, and research conducted by Boussouf et al. (2014) showed that R32 starts to burn spontaneously at 764°C, and when mixed with POE lubricating oil, it burns at 649°C; therefore, caution is needed when R32 is used. The properties of R32 are listed in Table 2. The critical temperature in R32 indicates the temperature limit when R32 is above the critical temperature and can no longer change the gas phase to liquid regardless of the pressure used. This is important because the critical temperature affects the system performance.

Table 2. General properties of R32 taken from Hwang et al. (2012)

No	Properties	Unit	R32
1	Chemical formula	-	CH ₂ F ₂
2	Composition	-	R32
3	Molecular weight	g/mol	52,0
4	Critical pressure	MPa	5,78
5	Critical temperature	°C	78,1
6	Boiling point	°C	-51,7
7	GWP	-	675

The testing stages in this study were divided into 2, namely testing in the refrigeration laboratory of the Renewable Energy Engineering Division of the Department of Mechanical Engineering and Biosystems, Bogor Agricultural University, and testing on a modified ship by PT Samudera Sinar Abadi Shipyards while on land and at sea. Both types of tests conducted in this study were no-load tests. Cold storage follows the refrigeration system in general, and consists of main components such as compressors, condensers, expansion valves, and evaporators. The specifications of the cold storage and photovoltaic systems are listed in Table 3. The compressor used was a compressor for R404a from Cubikel-type MPT18LA, which is now there is no R32 compressor available for low-temperature use

(cold storage). The compressor is based on specifications capable of working with evaporation temperatures up to -40°C and a working pressure of 3.8 MPa. The plan requirement in this research is an evaporation temperature of -28°C with a working pressure of up to 2.3 MPa so based on this, the R404a Cubikel MPT18LA compressor can be used. The thing from that needs to be considered in the use of this compressor is the oil change from R404a oil to R32 oil. The condenser and evaporator components are commonly used in cold storage using a forced convection type with a fan power of 43 Watt. The chamber component uses a sandwich panel type with the following material configuration and thickness: the first layer uses galvanized material with a thickness of 1 mm, the second layer uses polyurethane with a thickness of 10 mm, and the third layer uses galvanized material with a thickness of 1 mm. In addition, the power supply used photovoltaics. The use of photovoltaic is designed only to meet the energy needs for 8 h; the rest will use the ship's diesel engine, so that the electrical configuration can be seen in Figure 2. The photovoltaic cell used was a monocrystalline type with a power of 540 Wp and as many as two pieces. The inverter used was a hybrid type with a power of 3200 Watts. In addition to converting DC to AC, this Hybrid Inverter functions as a tool for switching electricity sources from photovoltaics or a ship's diesel engine.

Table 3. Component specifications of *cold storage*

No	Component	Specification	Description
1	Compressor	$\frac{3}{4}$ PK R404A hermetic type	Compressor with Hermetic type for R32 (low temperature) could not find in market.
2	Condenser	<i>Air Cooled condenser</i>	Equipped with fan by power consumption 43 Watt
3	Expansion Valve	<i>Needle valve</i>	TXV type for R32 with evaporation temperature -28°C couldn't find in the market
4	Evaporator	<i>Fine tube evaporator</i>	Equipped with fan by power consumption 43 Watt
5	<i>Chamber</i>	1,22 m x 1,41 m x 1,53 m	Sandwich Panel
6	<i>Control on-off</i>	PID	Temperature control in the chamber of <i>cold storage</i>
6	Inverter	Hybrid 3200 Watt	Convert DC to AC and controlled the power resource that used
7	<i>Photovoltaic</i>	2x540 Wp	Monocrystalline
8	Battery	2x(24V 200Ah)	VRLA (<i>Valve Regulated Lead Acid</i>) Gell Cell

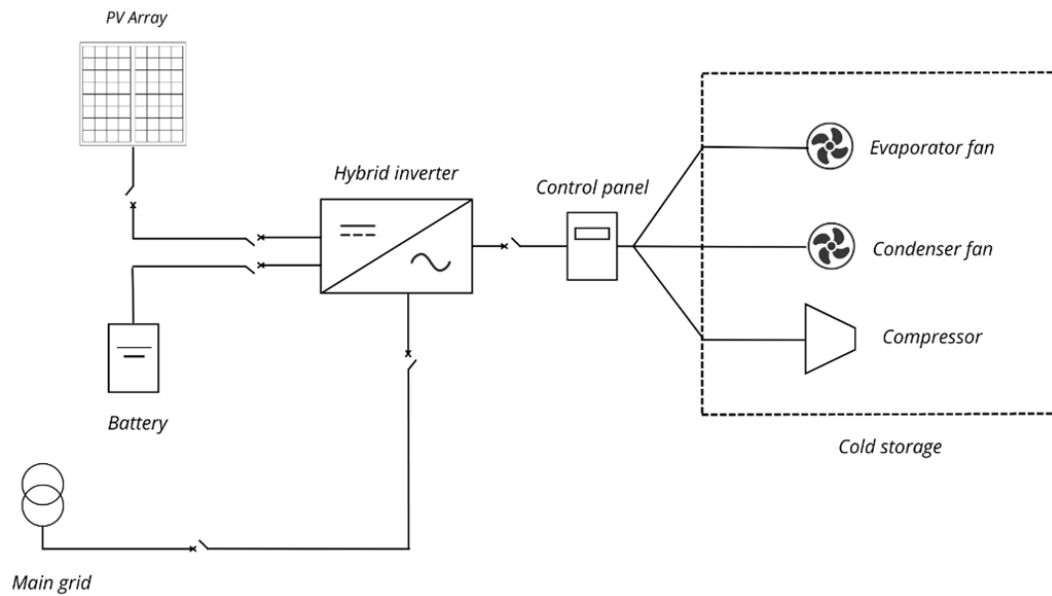


Figure 2. Electrical schematic of the Photovoltaic system used.

Figure 3 shows the experimental setup used for the cold storage testing in the laboratory. In the laboratory test, the pressure and temperature of each outgoing and incoming component were measured using a pressure transmitter and a K-type thermocouple with the number and distribution shown in Table 4. The compressor power was measured using a power meter and the refrigerant mass flow rate was measured using Coriolis.

All measurement data were connected to a data analyzer, which reads on a computer using software every 1 minute. Laboratory testing was conducted for 8.3 hours.



Figure 3. (a) Experimental setup for laboratory testing and (b) actual laboratory conditions.

Table 4. Amount and distribution of measure equipment

No	Measure equipment	Amount of measure equipment								
		Compressor		Condenser		Expansion valve		Evaporator		Chamber
		In	Out	In	Out	In	Out	In	Out	
1	Thermocouple type K	1	1	1	1	1	1	1	1	1
2	Pressure Transmitter	1	1	1	1	1	1	1	1	-
3	Coriolis	1	-	-	-	-	-	-	-	-
4	Power Meter		1	-	-	-	-	-	-	-

Figure 4 shows the experimental setup used in shipboard testing, both on land and in the sea lab. The refrigerant mass that was input into the system was 220 g for all tests in the lab, ship on land, and ship at sea. In testing on the ship, only the temperature of the chamber and the compressor power consumption during the cold storage machine operation were considered. Onboard testing was conducted for 24 h when the vessel was on land and for 5.3 hours when the vessel started to sail from land to the fishing spot.

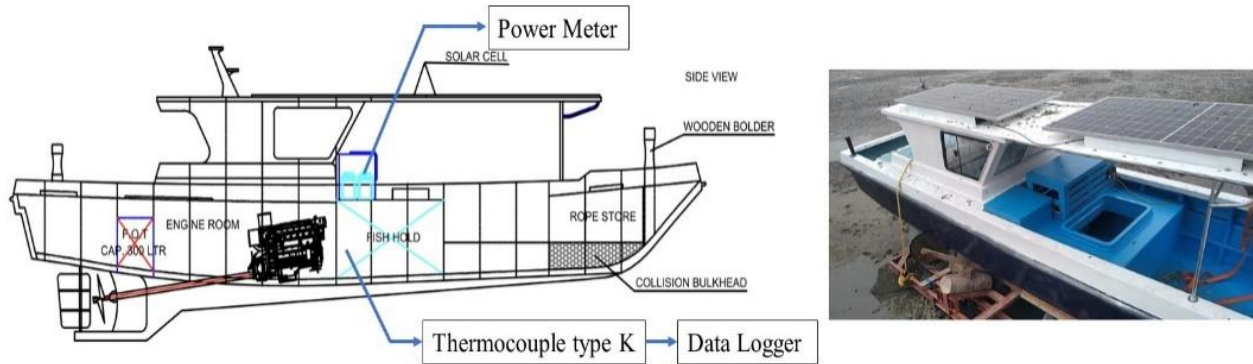


Figure 4. (a) Experimental setup of ship and (b) actual ship conditions.

The analysis of the cold-storage test results was based on the thermodynamic analysis described by Cengel and Boles (2015) and Ashrae (2014). The refrigerant flowed into the evaporator, and evaporation occurred. In this evaporation process there is an absorption of heat from the environment by (Q_e). The amount of heat absorbed by the evaporator depends on the refrigerant mass flow rate (\dot{m}) and the enthalpy change that occurs at the inlet side of the evaporator (h_4) and evaporator exit (h_1) the formula applies :

$$\dot{Q}_e = \dot{m}(h_1 - h_4) \tag{1}$$

The next process is an isentropic compression process, in which the refrigerant that comes out of the evaporator enters the compressor and is then compressed. In this process, a compressor was (\dot{W}_c) required. The work of the compressor is influenced by the mass flow rate entering the compressor and the enthalpy change entering the compressor. (h_1) compressor exit (h_2) in this process the fluid exiting the compressor is in the advanced hot vapor condition. The isentropic compression process can be mathematically expressed as follows:

$$\dot{W}_c = \dot{m}(h_2 - h_1) \quad (2)$$

After compression, the refrigerant enters the condenser. In the condenser, heat is dissipated from the system to the environment so that the refrigerant changes phase from hot vapor to liquid saturation. The amount of heat discharged into the environment (Q_c) influenced by the refrigerant flow rate (\dot{m}) and the incoming enthalpy change (h_2) and exit (h_3) condenser. Mathematically, this can be expressed as follows:

$$\dot{Q}_c = \dot{m}(h_2 - h_3) \quad (3)$$

The final process is the expansion process that occurs in the expansion valve. In this process an isoenthalpy process occurs where the enthalpy that enters (h_3) and exit (h_4) is the same, so materially it can be written as follows.

$$h_3 = h_4 \quad (4)$$

The performance of a vapor compression cooling system is expressed in COP (Coefficient of Performance) which depends on the ability of heat that can be absorbed by the evaporator in the room (Q_e) with the work required for the compression process (\dot{W}_c) which can be mathematically written as follows.

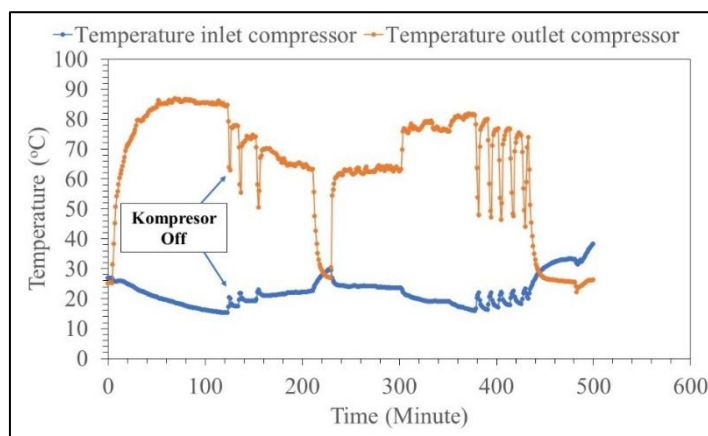
$$COP = \frac{\dot{Q}_e}{\dot{W}_c} = \frac{h_1 - h_4}{h_2 - h_1} \quad (5)$$

3. Result and Discussion

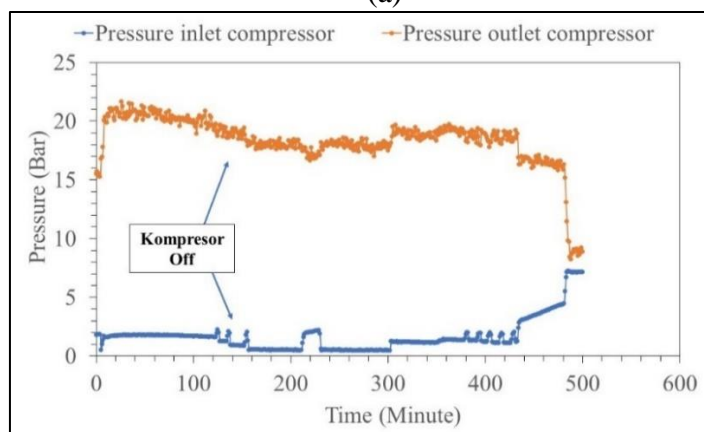
3.1 Temperature, Pressure and Power Consumption Profile

The first test was cold-storage testing at the Refrigeration Laboratory of the Renewable Energy Engineering Division of Bogor Agricultural University. Cold storage with R32 refrigerant and an energy source from photovoltaics is equipped with an on-off control on the cold storage system. The on-off system uses the input of the reach temperature of the chamber or the room being cooled. If the cooled room reaches a temperature of approximately -18°C , the compressor will turn off. The inlet and outlet temperature and pressure profiles of the compressor are shown in Figures 5 (a) and 5 (b),

respectively. As with vapor compression refrigeration systems, in general, the function of the compressor is to increase the temperature and pressure entering the compressor (suction). The compressor entry temperature is initially at about 25°C then after compression, the refrigerant temperature increases to approximately 95°C. The same phenomenon also occurs when the compressor outlet pressure (discharge) becomes 20 bar, whereas the compressor suction pressure is 1.9 Bar. The increase in temperature and pressure at the compressor exit is influenced by the amount of cooling load and refrigerant mass entering the system (mass charge), as revealed by Yulianto et al. (2024) for heat pump applications, and Hu et al. (2017) used R404a in cold storage. A higher cooling load and refrigerant mass cause an increase in the compressor outlet temperature and pressure. After the temperature in the chamber dropped owing to the heat absorbed by the refrigerant, the cooling load decreased, which caused the compressor pressure to gradually drop to approximately 18 bar at approximately 120 min. The machine was shut down at 120 min because the temperature in the chamber reached -18°C.



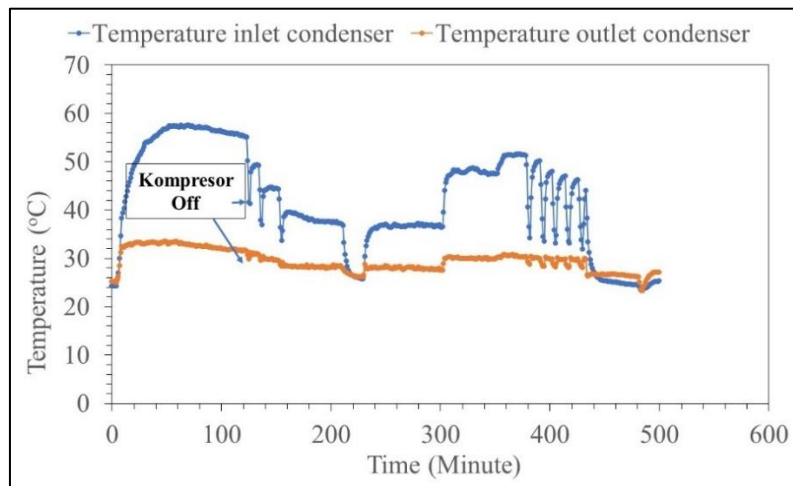
(a)



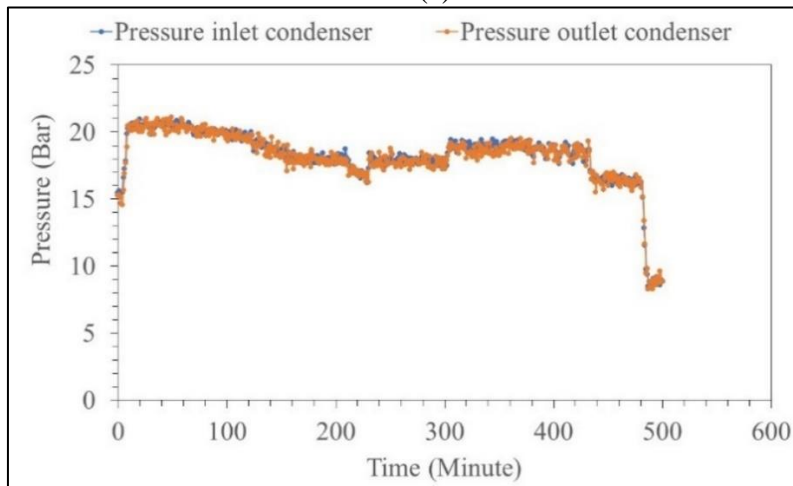
(b)

Figure 5. Compressor temperature and pressure profiles: (a) inlet and (b) outlet.

The next process after the refrigerant is compressed is the heat-dissipation process in the condenser. Figures 6 (a) and (b) show the temperature and pressure profiles at the condenser, respectively. In the condenser, the heat dissipation process from the refrigerant to the environment occurs at a constant pressure such that the temperature coming out of the condenser decreases from 57°C to 32°C., as shown in Figure 6(a). The greater the heat dissipated by the condenser, the lower the output temperature of the condenser, which indicates a well-performing condenser. Meanwhile, Figure 6 (b) shows that the inlet and outlet pressure profiles of the condenser are the same at 18-20 Bar so which proves that in the condenser, there is a decrease in temperature owing to the heat dissipation process to the environment at constant pressure, which is also in line with Hu et al. (2021) for the case of isothermal compression.



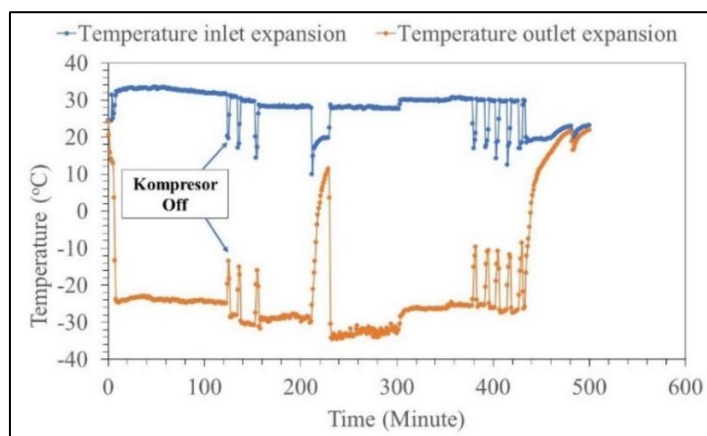
(a)



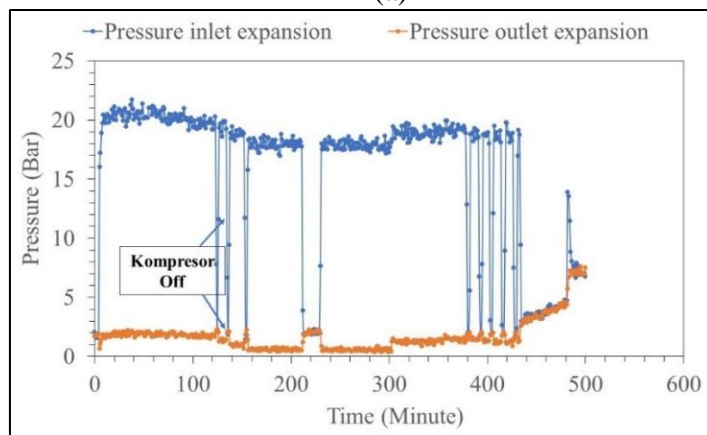
(b)

Figure 6. Condenser temperature and pressure profiles: (a) In and (b) Out.

The next step involved the expansion process. The expansion process occurs in the expansion valve, and the refrigerant decreases in temperature and pressure, as stated by Cengel et al. (2015) and Moran et al. (2018), as shown in Figure 7 (a) and (b). In Figure 7 (a), it can be seen that the inlet temperature of the expansion valve is 32°C then after exiting the expansion valve it becomes -28°C. With a target room temperature of -18°C, the minimum target evaporation temperature for R32 was -28°C. The evaporation temperature can only be achieved if the refrigerant pressure out of the expansion valve can reach 1.3-1.9 Bar in accordance with the refrigerant properties in REFPROP Ver 10.1 (Refrigerant). In this study, the expansion valve used a needle valve so that it was easy to adjust the desired pressure. In actual applications, expansion valves typically use thermal expansion valves (TXV) and capillaries. However, until now, TXV valves for R32 up to this pressure have not been available, so a possible alternative for actual applications can use capillary pipes. To calculate the dimensions of the capillary pipe, the inlet and outlet pressure information in Figure 7 (b) can be used as a reference.



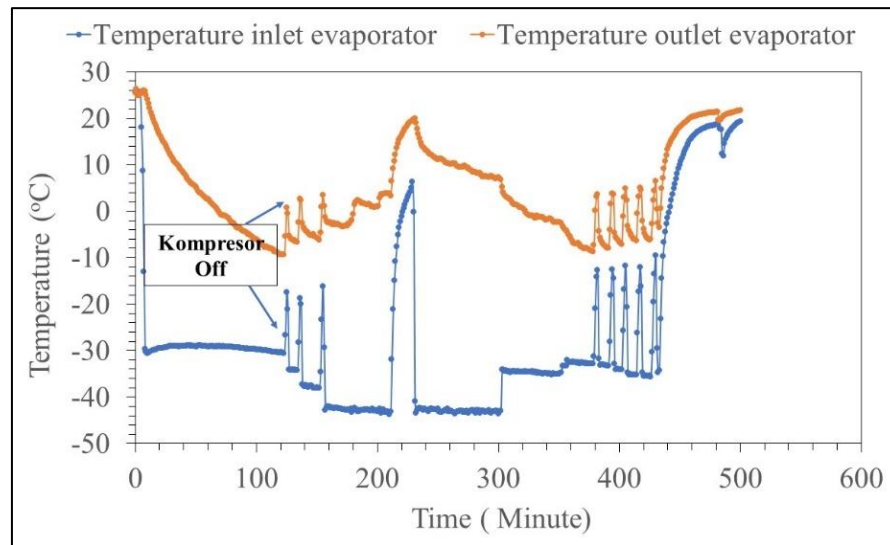
(a)



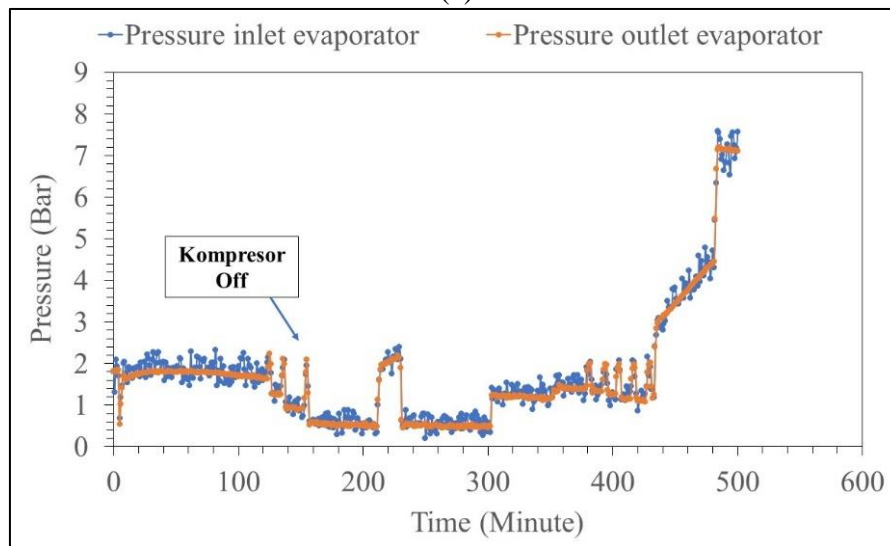
(b)

Figure 7. Expansion valve temperature and pressure profiles: (a) In, (b) Out

Figure 8 shows the temperature and pressure profiles of the evaporator. The evaporation process occurs in the evaporator because the refrigerant absorbs heat from the room to be cooled, according to the existing theory revealed by Cengel et al. (2015) and Moran et al. (2018). In Figure 8 (a), it can be seen that there is an increase in temperature on the exit side of the evaporator, the evaporator entry temperature that occurs is between -30°C to -40°C and the exit temperature is -9°C . The increase in temperature at the exit of the evaporator indicated the absorption of heat from the room to be cooled. The temperature change was at a fixed pressure condition of 1.6 to 1.8 Bar as shown in Figure 8 (b).



(a)



(b)

Figure 8. Evaporator temperature and pressure profiles: (a) In, and (b) Out.

Figure 9 shows the profile of the room temperature (a), power, and energy (b) of the cold storage tested in the refrigeration laboratory. The cold storage room temperature can reach -18°C according to the design target. The power required by the compressor to work is approximately 0.653 kW , with a total amount of energy during 500 min of operation of 3.87 kWh . At 200 min , it was difficult for the room temperature to reach the target temperature because of the ice block formed in the evaporator; thus, heat absorption in the room was inhibited. This cold storage was also equipped with a heater in the evaporator to remove the ice block formed in that section. From minute 200 to minute 230 , the defrost is turned on so that the chamber temperature increases to 15°C .

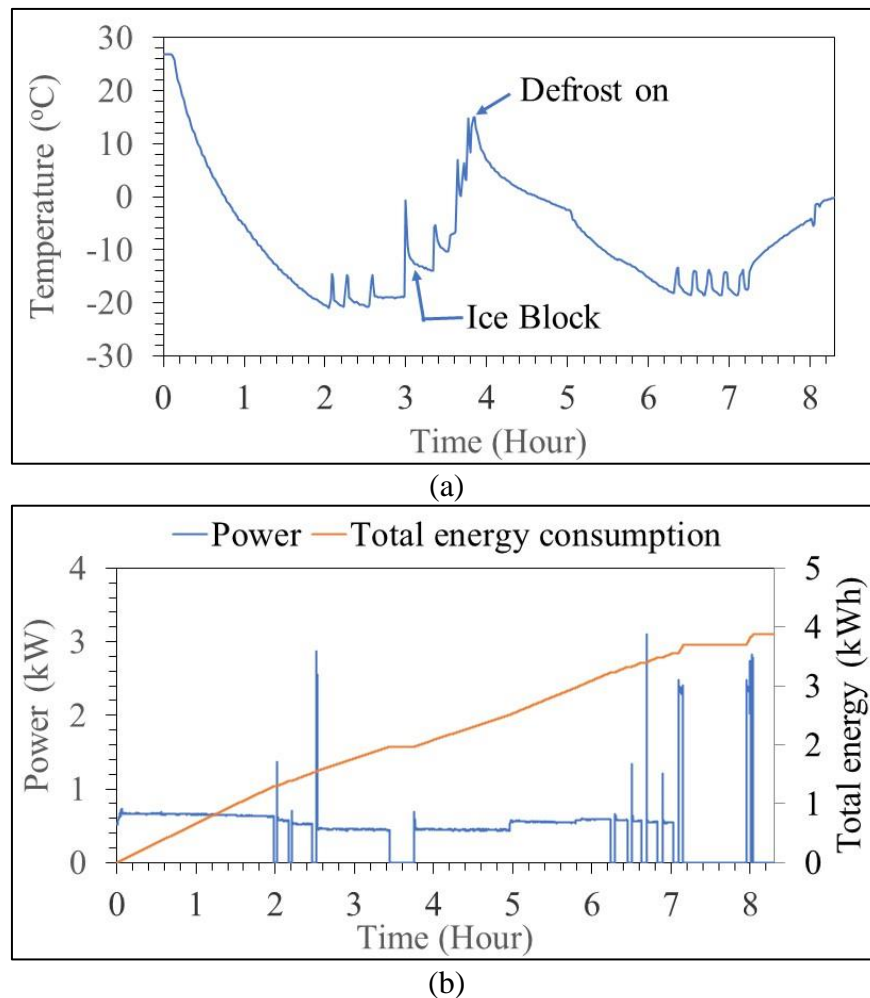


Figure 9. Temperature and power profiles in the laboratory: (a) CS room temperature and (b) power.

As explained in the method, cold storage testing is also carried out on the ship when the ship is on land and the ship is at sea, but the data taken onboard are only room temperature data and the total power and energy required during cold storage operations. Figure 10 shows the profile of the

room temperature (a), power, and energy (b) of the cold storage system tested on the ship while still on land. The test was conducted for 24 hours. Similarly, testing in the laboratory showed that the chamber temperature can reach -18°C with a compressor power requirement of 0.776 kW and total energy during cold storage operation of 11.48 kWh.

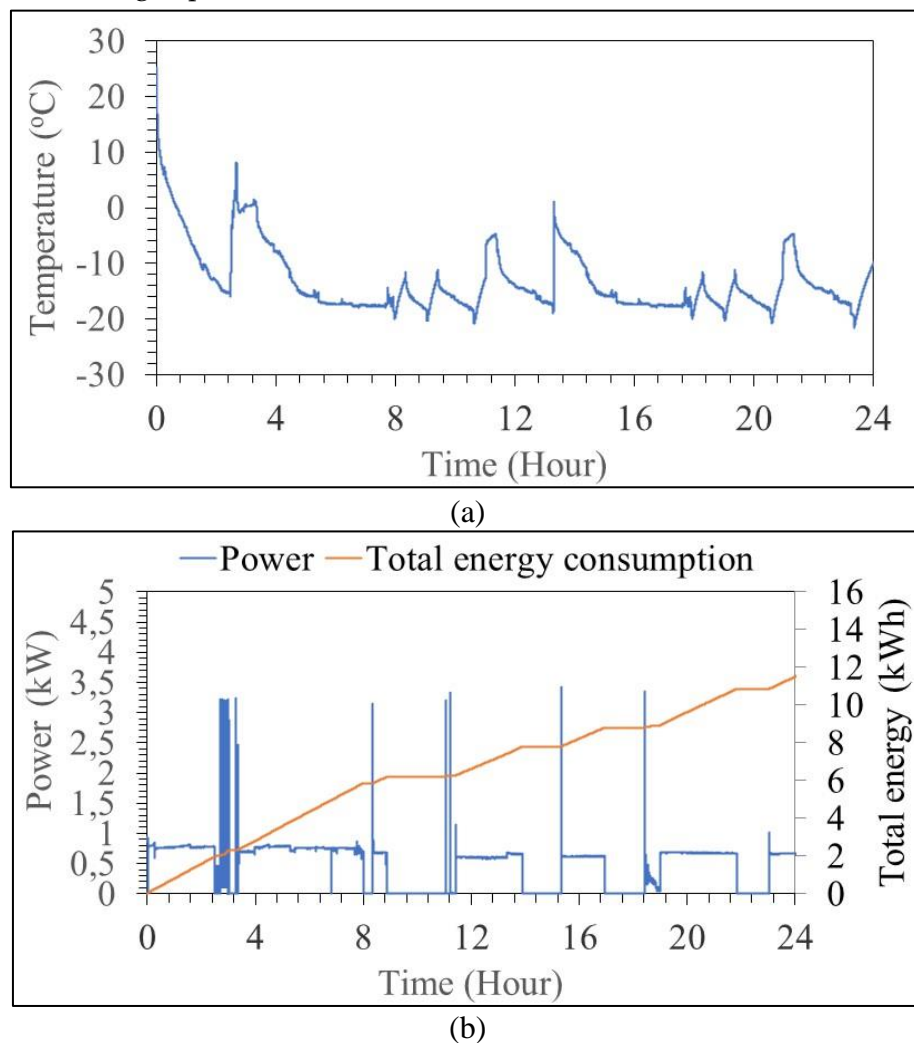


Figure 10. Temperature and power profiles on board: (a) CS room temperature and (b) power.

Figure 11 shows the profiles of room temperature (a), total power and energy (b) of the cold storage tested on the ship while operating at sea. At the temperature of the cold storage test achievements on the ship at sea can reach -18°C . Cold storage takes a longer time (approximately 4.5 h), even though cold storage testing is carried out at night according to the actual conditions when fishermen go to sea. This is because of several factors, including the air humidity that occurs on ships that have a larger cooling load. Another possibility is that the amount of mass charge entering cold storage is not yet

under optimum conditions. The power required for the cold storage to operate is approximately 0.75 kW with a total amount of energy required of 2.8 kWh.

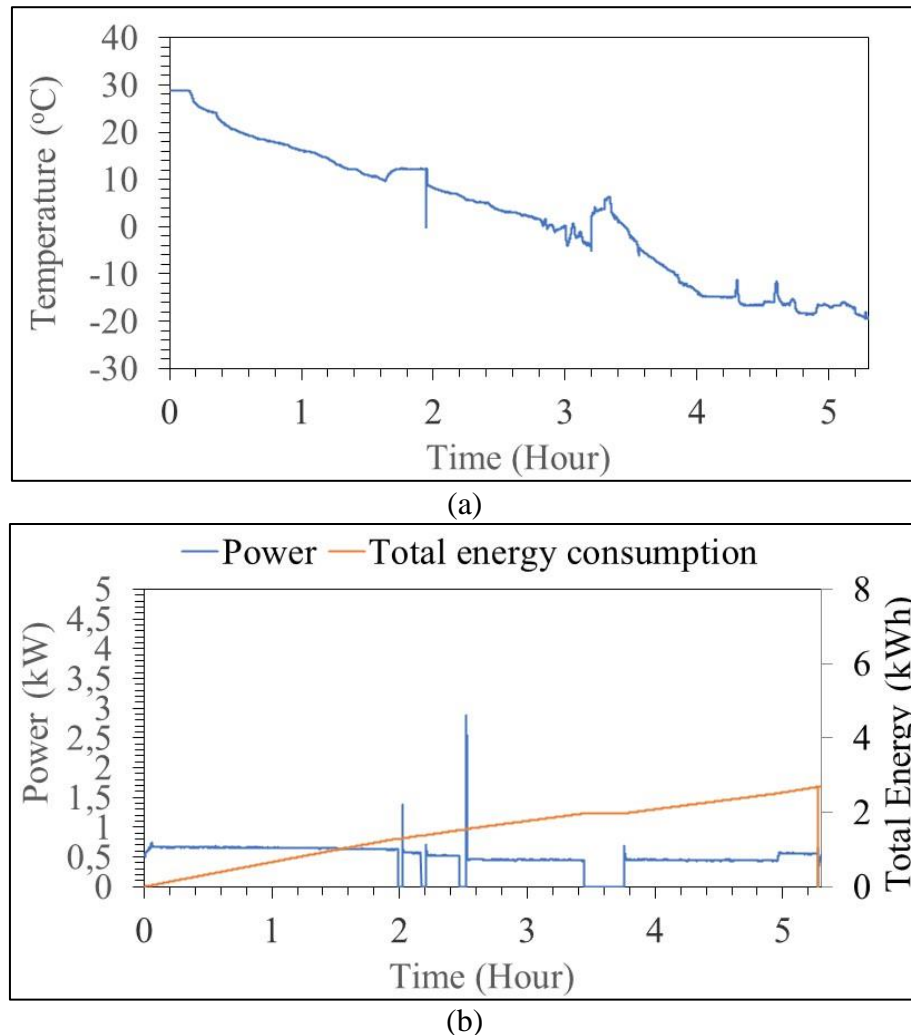


Figure 11. Temperature and power profiles on board: (a) CS room temperature and (b) power.

The energy needs used by cold storage with a vapor compressor cooling system in Figure 9-10, were supplied from the installed photovoltaic system. The amount of photovoltaic installed was 2×540 Wp with the ability to generate a peak electrical power of 1080 Watt so that it could meet 8 h of vapor compression cold storage operation needs with R32 refrigerant, the rest was supplied by PLN, and the ship's diesel engine was integrated into the hybrid inverter.

3.2 Analysis of Cold Storage With Refrigerant R32

Several analyses have been conducted to evaluate the performance of vapor compression refrigeration systems, including P-h diagrams, cooling capacity, and COP. Figure 12 shows the P-h

diagram generated during the cold storage test in the refrigeration laboratory. In the figure, it can be seen that processes 1 to 2 are isotropic compression processes, and R32 is able to produce a compressor discharge pressure of 20.6 Bar (2.06 MPa) with an enthalpy value of 586 kJ/kg.°C. The compressor inlet temperature touches the superheated condition with a superheated temperature (TSH) of 55.08°C. Processes 2–3 are the heat dissipation process. In this process, the condenser exit temperature, i , was 32°C, with an enthalpy of 259 kJ/kg. °C and a temperature sub cooling (TSC) of 0°C. The next process is from 3 to 4 which is called the expansion process. In the expansion process, the pressure difference capable of being generated by the needle valve as an expansion valve is 18.8 bar from an inlet pressure of 20.6 bar (2.06 MPa). In processes 4–1, namely, the evaporation process with an enthalpy change of 273 kJ/kg. the P-h cycle that occurs is based on the theory proposed by Cengel et al. (2-15), Moran et al. (2018), and Hu et al. (2017).

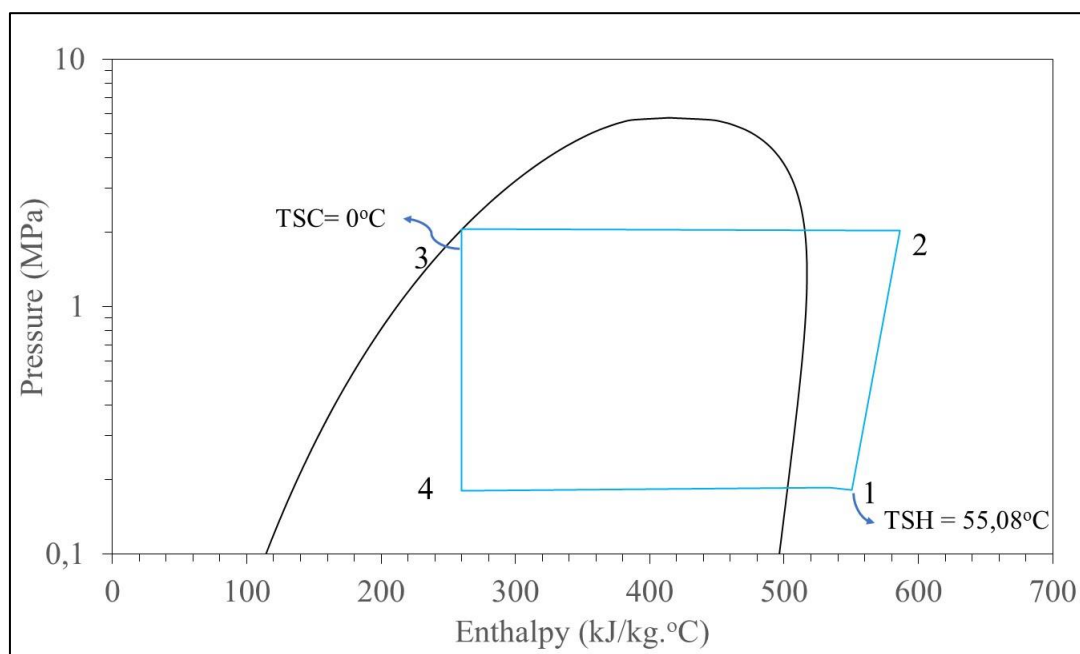


Figure 12. P-H analysis of R32 cold storage diagram.

In table 5 is a further analysis to determine the refrigerant mass flow rate, cooling capacity, heat dissipation to the environment, and COP (Coefficient of Performance) for cold storage testing in the refrigeration laboratory. It can be observed from the table that the refrigerant mass flow rate that carried and dissipated heat in the evaporator and condenser was 0.018 kg/s. With this flow rate, the R32 cold storage system made is able to dissipate heat from the condenser to the environment by 5.94 kW. While the cooling capacity of cold storage or the ability of the system to take heat in a room cooled with R32 refrigerant is 4.97 kW or equivalent to 16958.34 BTU/h. In general, the performance of R32

cold storage can produce a significant COP of approximately 7.62, which means that the cooling capacity that can be produced by R32 cold storage is 7.62 times the required compressor power consumption. The COP value for the use of R32 in this cold storage system was almost the same as the COP range revealed by Bhamidipati et al. (2020) for air conditioning systems and Yulianto et al. (2022) for the heat pump system.

Table 4. Performance of R32 cold storage system

No	Evaluation Parameter	Value
1	Mass flowrate (\dot{m})	0,018 kg/s
2	Cooling Capacity (\dot{Q}_e)	4,98kW
3	Heat Rejection (\dot{Q}_c)	5,94kW
4	COP	7,62

4. Conclusion

Vapor compression cold storage with R32 refrigerant with a photovoltaic energy source was fabricated and tested under no-load conditions in the refrigeration laboratory and on a ship modified by PT Samudera Sinar Abadi Shipyard.

The test results in the lab show that the R32 vapor compression refrigeration system for cold storage applications is able to cool the cold storage room at approximately $-18^{\circ}C$ with power consumption ranging from 0.65. Analysis of the cooling capacity that can be produced with a design evaporation temperature of $-28^{\circ}C$ of 16958.34 BTU / h with a Coefficient of Performance (COP) value of 7.62. The total energy requirement for 8.3 hours of testing in the lab amounted to 3.87 kWh.

The results of cold storage testing with a vapor compression refrigeration system using R32 onboard when the ship is still ashore are able to cool the cold storage room at approximately $-18^{\circ}C$ with a power of 0.77 kW. This test was conducted for 24 h, with a total energy consumption of 11.48 kWh.

The test results in the actual environment at sea show that the cold storage vapor compression system can cool the cold storage room at approximately $-18^{\circ}C$ for 4.7 hours with a power of 0.66 kW. The energy requirement during cold storage at sea for 5.3 hours of operation is 2.68 kWh.

All energy needs during testing in the lab, ships on land, and ships at sea use energy generated from photovoltaics with 2×540 Wp specifications that can last up to 8 h of operation; the rest use PLN and Diesel Engines for ships that have been integrated in hybrid inverters. Based on the test results, it can be concluded that Refrigerant R32 can be used for cold storage with a photovoltaic energy source.

Acknowledgement

We thank the Directorate of Higher Education, Research, and Technology and PT Samudera Sinar Abadi Shipyard through the 2023 kedaireka grant with contract number 31/E1/HK.02.02/2023 for funding this research.

5. References

- ASHRAE. (2014). *Ashrae handbook - Refrigeration*. Atlanta: ASHRAE.
- Arianto., M.F.,(2020). Potensi Wilayah Pesisir di Negara Indonesia. *J Geogr*. 20(20):1–7.
- Arief MI, Makhsud A, Sungkono. (2021). Perancangan cold storage berkapasitas 1 ton pada kapal nelayan tradisional. *J-Move : Jurnal Teknik Mesin*. 3(1):40-55. <https://doi.org/10.36289/jtmi.v17i2.302>
- American Society of Heating, R. and A.-C. Engineers., & American Society of Heating, R. and A.-C. Engineers. (n.d.). *2014 Ashrae handbook. Refrigeration*.
- Bhamidipati, A., Pendyala, S., & Prattipati, R. (2020). *Performance evaluation of multi pressure refrigeration system using R32*. *Materials Today: Proceedings*, 28, 2405–2410. <https://doi.org/10.1016/j.matpr.2020.04.716>
- Cabello, R., Sánchez, D., Llopis, R., Andreu-Nacher, A., & Calleja-Anta, D. (2022). Energy impact of the Internal Heat Exchanger in a horizontal freezing cabinet. Experimental evaluation with the R404A low-GWP alternatives R454C, R455A, R468A, R290 and R1270. *International Journal of Refrigeration*, 137, 22–33. <https://doi.org/10.1016/j.ijrefrig.2022.02.007>
- Cengel, Y. A., & Boles, M. A. (2015). *THERMODYNAMICS: AN ENGINEERING APPROACH, EIGHTH EDITION*.
- Fachrudin, F., & Aliredjo, S. (2021). Chilling System Insulation Hatch Design Using Refrigeration For 3GT Sized Vessels. *International Journal of Advanced Engineering Research and Science (IJAERS)*, 8(2), 2456–1908. <https://doi.org/10.22161/ijaers>
- Giriprasath, B. S., Chandramohan, R., Kumar, R. A., & Arun, N. K. (2021). Energy enhancement of air conditioner using R32 and R290 refrigerants. *AIP Conference Proceedings*, 2317. <https://doi.org/10.1063/5.0036221>
- Hadi, S. W., Tomy Wijaya, Y., Elysabeth, I. R., Aisyah, N., Dhimas, R., Putra, D., & Ariyadi, H. M. (2023). Energy performance analysis of r32 and r134a refrigerant for spring pool water heater. *Advanced Engineering Letters*, 2(3), 88–95. <https://doi.org/adeletters.2023.2.3.2>
- Hidayatno, A., Setiawan, A. D., Wikananda Supartha, I. M., Moeis, A. O., Rahman, I., & Widiono, E. (2020). Investigating policies on improving household rooftop photovoltaics adoption in Indonesia. *Renewable Energy*, 156(2020), 731–742. <https://doi.org/10.1016/j.renene.2020.04.106>

- Hu, X., Zhang, Z., Yao, Y., & Wang, Q. (2017). Experimental Analysis on Refrigerant Charge Optimization for Cold Storage Unit. *Procedia Engineering*, 205, 1108–1114. <https://doi.org/10.1016/j.renene.2020.04.106>
- Hu, Y., Xu, W., Ren, T., Cai, M., Yang, B., & Shi, Y. (2021). Theoretical study on the application of isothermal compression technology in vapor-compression refrigeration systems with an isothermal piston. *Energy Science and Engineering*, 9(12), 2321–2332. <https://doi.org/10.1002/ese3.984>
- Hwang, Y., Xu, X., Radermacher, R., & Pham, H. (2012). Performance Measurement of R32 Vapor Injection Heat Pump System. *International Refrigeration and Air Conditioning Conference*, 1–10.
- Moran MJ, Shapiro HN, Boettner DD, Bailey MB. 2018. *Fundamentals of Engineering Thermodynamics* 9 edition. Wiley.
- Natarajan B, Kathiresan AC, Subramaniam SK. (2023). Development and performance evaluation of a hybrid portable solar cold storage system for the preservation of vegetables and fruits in remote areas. *Journal of Energy Storage*. 72. <https://doi.org/10.1016/j.est.2023.108292>
- Nengah Ardita, I., Gusti Agung Bagus Wirajati, I., & Dewa Made Susila, I. (2021). Performance analysis of retrofit R410a refrigerant with R32 refrigerant on a split air conditioner. *Journal of Applied Mechanical Engineering and Green Technology*, 2, 1–04. <http://ojs.pnb.ac.id/index.php/JAMETECH>
- Nurhasanah R, Sudarmadi A. 2019. Perencanaan cold storage untuk pengawetan daging sapi PT. Kepurun Pawana Indonesia. *Power Plant*. 1(1):55-60.
- Pattana, S., Tantakitti, C., & Wiratkasem, K. (2020). Energy saving in six doors walk-in cooler. *Energy Reports*, 6, 510–515. <https://doi.org/10.1016/j.egy.2019.11.111>
- Prayudi, dan suhengki, J., & Teknik Mesin STT PLN Jakarta. (2017). Pengaruh beban pendingin terhadap kinerja mesin pendingin dengan refrigerant r134a dan mc134. *Jurnal Power Plant*, 4(4).
- Preston, J., Kelautan, S. P., Dumai, P., Sekolah, M. M., & Perikanan, T. (2018). Analysis of Thermodynamic refrigeration cycle : Optimisation of heat transfer rate by Pilot Control Servo ICS Valve on Pulse Width Modulation Scheme. *Article in International Journal of Basic & Applied Sciences*. <https://doi.org/10.5281/zenodo.1473873>
- Saito, K. (2017). *Latest heat pump technologies in Japan*. 12th IEA Heat Pump Conference.
- Shi, H., & Wu, J. (2019). The Performance Analysis of R32 Rotary Compressor Used for Room Air Conditioners. *IOP Conference Series: Materials Science and Engineering*, 604(1). <https://doi.org/10.1088/1757-899X/604/1/012082>
- Yang, L., Villalobos, U., Akhmetov, B., Gil, A., Khor, J. O., Palacios, A., Li, Y., Ding, Y., Cabeza, L. F., Tan, W. L., & Romagnoli, A. (2021). A comprehensive review on sub-zero temperature cold thermal energy storage materials, technologies, and applications: State of the art and recent

developments. In *Applied Energy* (Vol. 288). Elsevier Ltd. <https://doi.org/10.1016/j.apenergy.2021.116555>

Yulianto, M., Giannetti, N., Miyaoka, Y., Ge, Z., Tsuchino, T., Urakawa, M., Taira, S., Jeong, J., & Saito, K. (2024). Effect of refrigerant charge on the performance and environmental footprint of R32 heat pump water heater. *AIP Conference Proceedings*, 2836(1). <https://doi.org/10.1063/5.0207267>

Yulianto M, Suzuki T, Ge Z, Tsuchino T, Urakawa M, Taira S, Miyaoka Y, Giannetti N, Li L, Saito K. (2022). Performance assessment of an R32 commercial heat pump water heater in different climates. *Sustainable Energy Technologies and Assessments*. 49. <https://doi.org/10.1016/j.seta.2021.101679>

Zheng, H., Tian, G., Zhao, Y., Jin, C., Ju, F., & Wang, C. (2022). Experimental study of R290 replacement R134a in cold storage air conditioning system. *Case Studies in Thermal Engineering*, 36. <https://doi.org/10.1016/j.csite.2022.102203>